Distributions of single-molecule properties as tools for the study of dynamical heterogeneities in nanoconfined water

2014 J. Phys.: Condens. Matter 26 155103

(http://iopscience.iop.org/0953-8984/26/15/155103)

IOP Publishing Journal of Physics: Condensed Matter
J. Phys.: Condens. Matter **26** (2014) 155103 (14pp) doi:10.1088/0953-8984/26/15/155103

Distributions of single-molecule properties as tools for the study of dynamical heterogeneities in nanoconfined water

G B Suffritti[1], P Demontis[1], J Gulín-González[2] and M Masia[1,3]

[1] Dipartimento di Chimica e Farmacia, Università di Sassari and INSTM, Unità di ricerca di Sassari, Via Vienna 2, I-07100 Sassari, Italy
[2] Grupo de Matemática y Física Computacionales, Universidad de las Ciencias Informáticas (UCI), Carretera a San Antonio de los Baños, Km 21/2, Torrens, La Habana, Cuba

E-mail: pino@uniss.it

Received 29 October 2013, revised 3 February 2014
Accepted for publication 12 February 2014
Published 27 March 2014

Abstract
The explicit trend of the distribution functions of single-molecule rotational relaxation constants and atomic mean-square displacement are used to study the dynamical heterogeneities in nanoconfined water. The trend of the single-molecule properties distributions is related to the dynamic heterogeneities, and to the dynamic crossovers found in water clusters of different shapes and sizes and confined in a variety of zeolites. This was true in all the cases that were considered, in spite of the various shapes and sizes of the clusters. It is confirmed that the high temperature dynamical crossover occurring in the temperature range 200–230 K can be interpreted at a molecular level as the formation of almost translationally rigid clusters, characterized by some rotational freedom, hydrogen bond exchange and translational jumps as cage-to-cage processes. We also suggest a mechanism for the low temperature dynamical crossover (LTDC), falling in the temperature range 150–185 K, through which the adsorbed water clusters are made of nearly rigid sub-clusters, slightly mismatched, and thus permitting a relatively free librational motion at their borders. It appears that the condition required for LTDC to occur is the presence of highly heterogeneous environments for the adsorbed molecules, with some dangling hydrogen bonds or weaker than water–water hydrogen bonds. Under these conditions some dynamics are permitted at very low temperature, although most rotational motion is frozen. Therefore, it is unlikely, though not entirely excluded, that LTDC will be found in supercooled bulk water where no heterogeneous interface is present.

Keywords: nanoconfined water, dynamical crossovers, molecular dynamics simulation, distributions of molecular properties

(Some figures may appear in colour only in the online journal)

1. Introduction

Dynamical heterogeneities in bulk and confined water have been studied and discussed for more than a century. Indeed, it is well known that the hypothesis that water is a mixture of two liquids, with different structures of the same chemical composition, was proposed by Röntgen in 1892 [1]. Recent accounts of the still lively debate about water heterogeneities—and of the experimental, theoretical and computational investigations undertaken to unravel this complex topic—can be found in the literature [2–26] (we quote only some relevant examples). In simulation studies, a number of statistical tools have been proposed to dig out the signatures of dynamical heterogeneities in water, such as mean-square displacement (MSD) distributions [2, 4, 6, 7], hydrogen bond (HB)

[3] Present address: Institut für Physikalische und Theoretische Chemie, Goethe Universität Frankfurt, Max von Laue Str. 7, D-60438 Frankfurt am Main, Germany.

cooperativity and dynamics [6, 9, 12, 23–25], spatially correlated clusters [4,5], local density fluctuations and correlations [7–11, 22, 23], polarizability anisotropy correlation [15], mobility transfer function [17], statistics of correlate hopping [18,26], multi-scale displacement analysis [26], analysis of the free-energy landscape and order parameters [21]. In the present work *explicit distributions* of two single-molecule properties: the rotational relaxation constant (τ_2)—or, more precisely, for computational reasons discussed below, its inverse ($1/\tau_2$)—and MSDs of O and H atoms, are separately used to study dynamical heterogeneities in nanoconfined supercooled water adsorbed in zeolites, which are microporous crystalline aluminosilicates. Whereas in many investigations the analysis is mainly about the trend of thermodynamic or average quantities, we are focusing on the mechanisms which determine various dynamic behaviours and their crossovers at molecular level. In particular, single-molecule distributions yield more detailed information than averages or other collective distributions. For example, Gaussian distributions of $1/\tau_2$ can be caused only by an environment which is dynamically homogeneous (the rotational relaxations of any molecule occur in a characteristic time close to the average) and thus, on average, structurally homogeneous. As will be shown below, deviations from Gaussian-like trend are not only mono-modal asymmetric distributions, but also multimodal distributions which permit the picking out of the onset of dynamical heterogeneities. Single-particle MSD distributions of O atoms allow detection of the onset of diffusion jumps, even for a few molecules (which does not appear in average MSDs) and the excess distributions of H atoms, with respect to those of O atoms, evidence independent rotational and translational motions which are typical of a 'strong liquid' behaviour [24–26]. Conversely, if the distributions are superimposed at a molecular (square) diameter scale, there is a sign of concerted rotational–translational motion, characteristic of 'fragile liquid' behaviour [25], in particular in water [26–32]. The distribution of $1/\tau_2$ was already used in [33], but in qualitative form and only for water in silicalite. An explicit distribution of a similar quantity, the single-exponential decay times of the HB exchange correlation function (shortly, jump times), was evaluated in [24]. The distribution of oxygen's MSD was used by La Nave and Sciortino [2] to study dynamic heterogeneities in water and in several other papers (typical examples are [34, 35]) to investigate dynamic heterogeneities in a two-dimensional glass-forming liquid using, among others, the single-particle MSD. They evaluated these quantities for short times in order to pick out the dynamic behaviour of the particles belonging to the boundaries or to the bulk of clusters that are formed in a moderately supercooled liquid. Discussion of the trends of both quantities at different temperatures, and for different systems, allows confirmation and substantial deepening of the interpretation of the dynamical heterogeneities and dynamic crossovers in supercooled bulk and nanoconfined water proposed in [33]. Water adsorbed in zeolites is usually (but not always, see below) dynamically heterogeneous, in a natural way, because of the presence of confining surfaces and coordinating cations whose structure and characteristics are well known and are related to a crystalline order. Therefore, the correspondence of these heterogeneities with the trend of the single-molecule distributions allow validation of the information that they can convey and their application to disordered media and to bulk water.

In two previous papers [33, 36] we reported extensive classical molecular dynamics (MD) [37] simulations of different kinds of geometric arrangement of the water molecules adsorbed in zeolites. The zeolite structure is built from corner sharing TO_4 (T = Si, P, Al, Ga, etc) tetrahedral units, which are linked together to form a periodic framework of interconnecting cavities and channels of nanometric or sub-nanometric dimensions. Guest molecules, such as *water* and *cations* (usually metallic), which compensate for the charge deficit due to the aluminum/silicon (or, more generally, $T^{3+} \rightarrow T^{4+}$) substitutions can be accommodated in nanopores [38–40]. In our simulations we considered water adsorbed in zeolites with nanopores of various topology, shape and diameter, such as worm-like clusters (in silicalite [41]), spherical nano-clusters (in zeolite Na A and Ca A [42]), cross-linked nanowires (in Na X [43]), and ice-like nanotubes (in $AlPO_4$-5 and SSZ-24 [33, 36]). In all these cases, from MD simulations performed in the temperature range 110–350 K, dynamic crossover phenomena were found, in spite of the different shape and size of the clusters, even when the confinement hinders the formation of tetrahedral HBs for water molecules. As a gauge of the dynamic crossover of water the trend of rotational relaxation constants (τ_2) was used, as they are easier to evaluate than other dynamic quantities, such as diffusion coefficients—especially at very low temperature—and because they are sometimes available experimentally (via nuclear magnetic resonance (NMR) experiments). In addition, these constants are related to HB dynamics (forming, breaking and switching), which is one of the main factors determining dynamical heterogeneities in bulk water [6–9, 12, 15, 23–31] and in water confined in silica nanopores [24, 44], as well as in reverse micelles [45–47]. Favourable comparison with a number of experimental results permits us to put forward some hypotheses about the mechanisms underlying the dynamic crossovers of nanoconfined water at low temperature. As reported in [33, 36] two dynamical crossovers were found (see figure 1): high temperature dynamical crossover (HTDC), occurring in the temperature range 200–230 K, which can be interpreted at a molecular level as the formation of translationally almost rigid clusters, which allow, however, some rotational freedom, including HB exchange and translational jumps as cage-to-cage processes. The suggested mechanism for the low temperature dynamical crossover (LTDC), falling in the temperature range 150–185 K, is that the adsorbed water clusters be made of nearly rigid sub-clusters, slightly mismatched, which thus permit a relatively free librational motion at their borders. Supercooled water adsorbed in zeolites is interesting, because water cannot crystallize at any temperature. Indeed, zeolite cavity and channel sizes, at least in the cases that were considered, do not exceed 12.5 Å. On the other hand, it was found experimentally—for water clusters $(H_2O)_n$ included in reverse micelles [48], and in size-selected supercooled water clusters *in vacuo* [49]—that the limiting value of n to prevent crystallization is about 150 and 255,

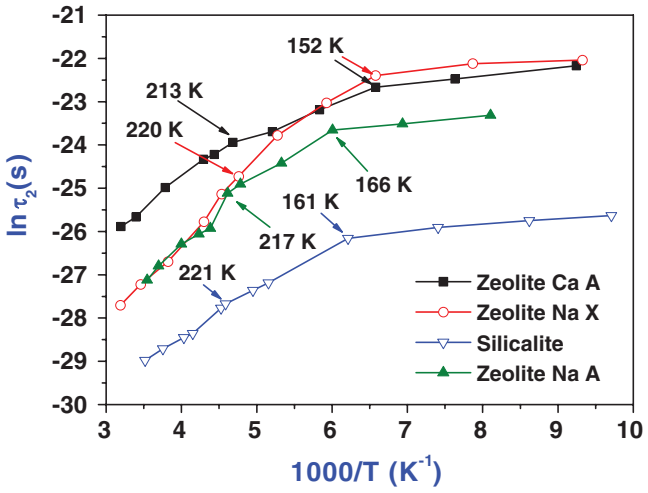

Figure 1. Arrhenius plot of the computed rotational relaxation constants, for water adsorbed in the considered zeolites. The arrows indicate the dynamical crossover temperatures.

respectively. For spherical clusters, this corresponds to about 20.5 and 25 Å in diameter.

From a computational standpoint, as zeolites are crystalline materials, channels and cavities are distributed periodically in space, so that periodic boundary conditions can be applied in a natural way without the need to simulate large systems. Obviously, the extrapolation of the behaviour of nanoconfined supercooled water to bulk water is not straightforward and should be discussed in detail. Discussion of the trends of both quantities, at different temperatures and for the different systems, will confirm and deepen the interpretation of the dynamical heterogeneities and dynamic crossovers in supercooled nanoconfined water. Our simulations were performed using classical mechanics, thus neglecting quantum effects, which become relevant especially at low temperatures, due essentially to the tunnel effect which enhances the mobility of the hydrogen atoms. As a result, when quantum effects are considered the computed values of diffusion coefficients, MSDs and rotational constants are larger by a factor that can reach one order of magnitude at very low temperatures [50–52]. This issue was discussed in a previous paper [36]. In fact, empirical potentials, such as the one used in the present work, are tuned to compensate, at least in part, for quantum effects. Indeed, the experimental values of HTDC for water adsorbed in zeolite Na X, 220 K [53–55] and in zeolite Ca A, 205 K [53]—the only available among the materials considered—and those resulting from our simulations [36]—220 K and 213 K, respectively—are well reproduced. On the contrary, the experimental temperatures of the LTDC are larger than the computed values, which are 152 K (185 K) and 152 K (165 K) for zeolite Na X and zeolite Ca A, respectively, the values in parenthesis being the experimental ones. This result is contrary to what was expected, because quantum effects should enhance the molecular mobility and cause the dynamical crossovers to fall at a lower temperature. Probably, the extra mobility of water found in the simulations could be ascribed to underestimated water–guest interactions, which are involved in inducing the LTDC in zeolites. In view of these uncertainties, the quantum corrections—which are demanding of computer resources—may not be necessary, and in the present study we shall content ourselves with classical MD yielding semi-quantitative results.

2. Method and calculations

Details of the MD simulations of water adsorbed in zeolites, and of the potential models adopted, are discussed in a previous paper [36]. Here we mention only the most relevant points. Classical MD simulations were performed in the microcanonical (*NVE*) ensemble in the temperature range 100–350 K and the production runs spanned a time range from 2 to 17 ns, depending on the system and on the temperature, so as to ensure the convergence of the quantities considered. A comment should be added about the different interactions involving the adsorbed water molecules. A zeolite pore surface is covered with oxygen atoms which are linked to Si or Al atoms lying behind them. Water molecules are connected to the surface oxygen by HBs, which however are weaker than water–water HBs. Indeed, all-silica zeolites, such as silicalite, are 'hydrophobic'—the adsorbed water prefers to form molecular clusters rather than to 'wet' the zeolite surface. When cations (which maintain their formal charge) are present on the surface, they coordinate the water molecules through interactions, which are stronger than water–water HBs. The coordinated molecules show a reduced mobility, both translational and rotational, especially when the cations are doubly charged, as in Ca^{2+}. A thorough discussion can be found in a previous paper [56], where computed and experimental diffusivities of water in zeolites A, containing different cations, are compared.

The rotational relaxation constants (τ_2) were evaluated by computing first the second-order rotational autocorrelation functions, averaged over all the water molecules of the system:

$$C_2(t) = \langle P_2[u(0)\cdot u(t)\,]\,\rangle\,, \qquad (1)$$

where $u(t)$ is the unit vector of the HOH plane, perpendicular to the plane (as usual in analytical geometry), and P_2 is the second-order Legendre polynomial. This autocorrelation function can be compared with the results of NMR experiments [57]. The rotational relaxation time τ_2 of water molecules was evaluated by fitting $C_2(t)$ to the sum of two exponential decays and by choosing the largest relaxation time constant. Indeed, it was found that a single exponential form was not sufficient for a good fit of $C_2(t)$. The smaller time constant value τ_1 is in the range 0.1–1 ps at room temperature and reaches some picoseconds at very low temperatures (less than 150 K). It can be interpreted as the relaxation time of the librational motion of the molecules. This interpretation was confirmed by Zasetsky [58], who analysed MD simulations of bulk water in the temperature range 240–340 K and identified three rotational relaxation constants. The smallest is of the order of 10^{-1} ps: it is nearly independent of temperature and it is related to bending (oscillatory) motion. The intermediate constant is of the order of 1 ps: this is moderately dependent on temperature and is ascribed to the large librational motions inside the rotational

potential well. Finally, the largest one (with values spanning from 2.6 ps for silicalite at room temperature to 260 ps for zeolite NaX at 107 K), which depends strongly on the temperature and thus corresponds to an activated process, involves the escape of the molecules from the rotational potential well, or the HB exchange [58]. We could distinguish between two constants only, because the smallest constants are out of reach of our simulations, as the shortest time interval between two coordinate savings in our simulations was of 0.032 ps. Saving the coordinates each step would result in too large files and too long times to evaluate the distributions, without yielding further useful information for the present work. *Single-molecule* rotational relaxation constants could be derived from equation (1), evaluated for each molecule separately, but the fitting procedure would have been unfeasible in practice because it cannot be calculated automatically by a simple and standard procedure. We note that, except for silicalite, where the adsorbed molecules are only 16, in the other considered cases they are in the range 219–250. As our discussion is semi-quantitative, it turned out to be easier and more straightforward to compute the quantity: $-\ln C_2(t_0)$, where t_0 is a time sufficiently long to make the term corresponding to the faster relaxation negligible. Indeed, if

$$C_2(t) = A_1 \exp(-t/\tau_1) + A_2 \exp(-t/\tau_2), \qquad (2)$$

then, for a sufficiently long time $t_0 >> \tau_1$, one has

$$\begin{aligned} -\ln C_2(t_0) &= -\ln[A_1 \exp(-t_0/\tau_1) + A_2 \exp(-t_0/\tau_2)] \\ &\approx -\ln A_2 + t_0/\tau_2, \end{aligned} \qquad (3)$$

so that the distribution of $-\ln C_2(t_0)$ is, qualitatively, that of $1/\tau_2$, which is the slope of $-\ln C_2(t_0)$ at sufficiently large t. Large values of $-\ln C_2(t_0)$ correspond to small values of τ_2 and then to high rotational mobility. An example will better illustrate the procedure to evaluate the distribution of $-\ln C_2(t_0)$. For hydrated silicalite, containing only 16 water molecules per simulation box, we calculated the rotational autocorrelation functions separately for each adsorbed molecule, and found that, for temperatures higher than 160 K, the trend of the single-molecule autocorrelation functions appears as a swarm of lines evenly distributed around the average (see figure 5 of [33]). For lower temperatures—as in figure 2(*a*), where T = 130 K—most of the autocorrelation functions exhibit a very slow decay, but some of them decay at a higher rate, similar to that observed at much higher temperature.

In order to make the discussion more quantitative and applicable to systems containing many water molecules, we fixed a reasonably large time t_0 (namely about 5 ps) and evaluated the distribution of $-\ln C_2(t_0)$ (see figure 2(*a*)). To assess this choice, we remark that the crucial point in the analysis of the considered distributions is a Gaussian-like or non-Gaussian-like behaviour, because the latter case is a clear indication of a dynamical heterogeneity. Although the single-molecule correlation functions visible in figure 2(*a*) show a relatively disordered trend, and cross each other at different times, it is possible to distinguish between ten of them remaining around the average, while six others are evidently far from the average.

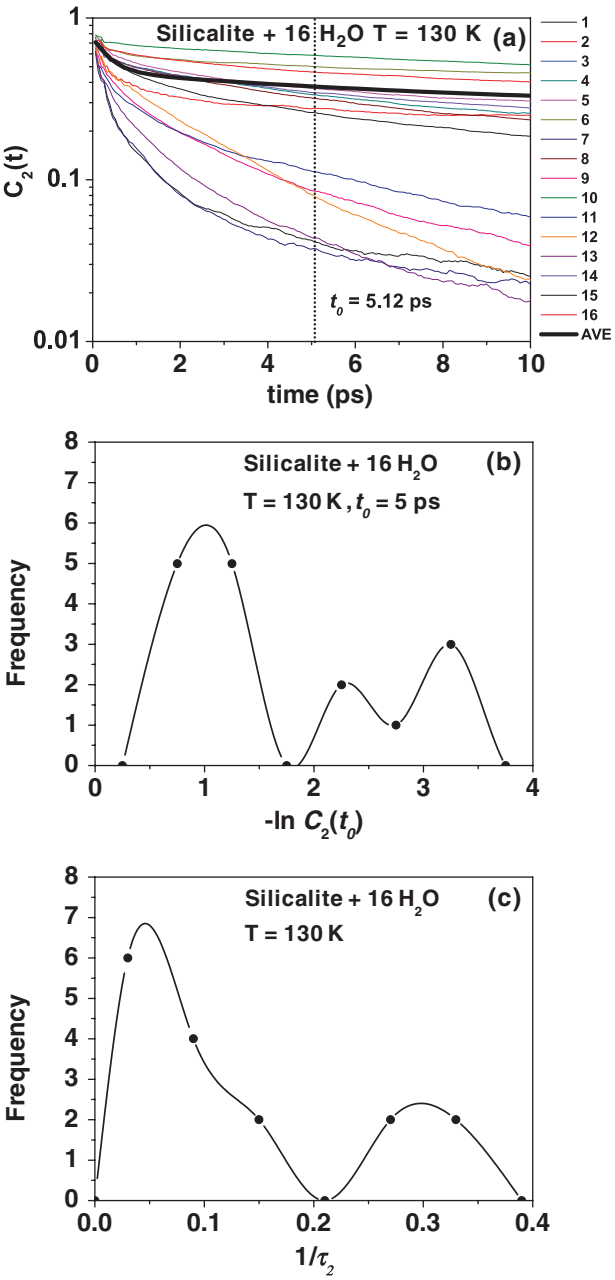

Figure 2. (*a*) Logarithmic plot of the computed single-molecule rotational relaxation autocorrelation functions for water in silicalite, at 130 K. The thick black line represents the average $C_2(t)$. The vertical dotted line crosses the single-molecule correlation functions at $t = t_0$. (*b*) Distribution of $-\ln C_2(t_0)$ along the vertical line in (*a*). Symbols represent the values of a histogram with bins having a width equal to 0.5. (*c*) Distribution of $1/\tau_2$, for which histogram with bins have a width equal to 0.06 ps^{-1}. Lines are to help guide the eye. In this figure, which has an illustrative scope, they are obtained by spline interpolation.

Correspondingly, the distribution plotted in figure 2(*b*) shows one Gaussian-like peak (or 'main' peak, because it includes the average value) and two extra smaller peaks, overall containing just six hits or molecules. We verified also that, by doubling the simulation box sides—thus including eight times molecules in the system—the shape of the distribution did not change appreciably. Another possible source of error is the histograms bins widths, which have been chosen in

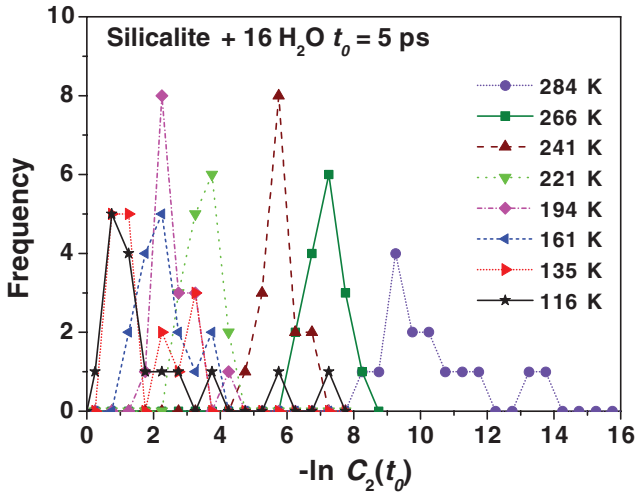

Figure 3. Distributions of $-\ln C_2(t_0)$ at different temperatures, for water in silicalite. Lines are to help guide the eye.

order to yield smooth main peaks. In all the cases that were considered, besides silicalite, the number of water molecules was in the range 219–250, and we found that a reasonable choice was to divide the range of the values of $-\ln C_2(t_0)$ into 20–30 bins. In conclusion, it is not straightforward to derive the overall exact errors in the distributions, but from a series of examples we ascertained that they did not change the appearance of the distributions themselves. Indeed, our analysis is based essentially on the relative importance and extension of the 'extra tails'.

The MSDs were evaluated for each O and H atom, thus allowing one to detect the decoupling of translational and rotational motion of the molecules, because after the slowing down and the arrest of the translations caused by lowering the temperature, some rotational motion can survive. For the choice of the bin width of the MSD distributions the same criteria as for those of $-\ln C_2(t_0)$ were adopted. In the figures, the bin height of the histograms are represented by symbols and are connected by straight lines to allow the reader to distinguish, and to compare, the different distributions. Bar plots turned out to be inadequate, and connecting the symbols with splines was attractive but possibly misleading. The last choice was used only in figure 3, where it was found that the poor statistics was not sufficient to render its illustrative character. Using another example would have entailed the cumbersome fitting of more than 200 correlation functions 'by hand' to derive the exact distribution of $1/\tau_2$. If we took $t_0 = 10$ ps, the related distribution would be qualitatively similar, the only difference being the exchanged heights of the two extra peaks, indicating that in both cases six molecules show a heterogeneous dynamical behaviour. This finding is confirmed by the 'true' distribution of $1/\tau_2$ in figure 2(*c*), where an extra peak, with four values, is evident and a shoulder in the larger peak allows us to guess at two other values not belonging to the main peak. Indeed, in the case of silicalite only 16 molecules are present and it was possible to evaluate the rotational relaxation constants for each molecule by the usual fitting procedure. The above discussion allows

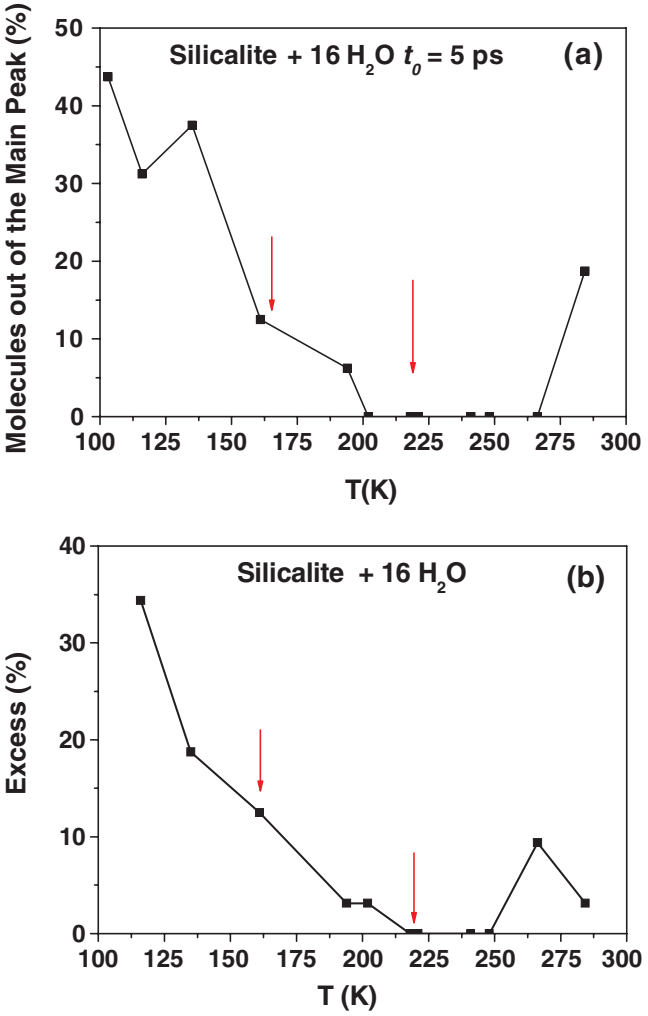

Figure 4. General trends of the distributions of single-molecule properties for silicalite. (*a*) Percentage of molecules showing values of $-\ln C_2(t_0)$ out of the main peak of the distribution against temperature, for water in silicalite. (*b*) Percentage of molecules showing a distribution of H atom MSDs larger than that of O atoms out of the main peak of the distribution against temperature. The red arrows show the dynamic crossover temperatures as derived from the Arrhenius plot of the rotational relaxation constants (see figure 1). Lines are to help guide the eye.

us to point out the source and the nature of the statistical errors in our treatment. Different choices of t_0 or the use of the approximation in equation (3) does not change substantially the behaviour or 'shape' of the distributions, which turn out to be sufficiently 'robust'.

3. Results and discussion

3.1 Silicalite

From MD simulations of hydrated silicalite, containing 16 water molecules per simulation box, reported in previous papers [36, 41], it results that at very low temperatures ($T < 200$–220 K) water appears to be mostly in the form of amorphous worm-like clusters among which a slow molecule interchange occurs, giving rise to a single-file-like diffusion on the timescale of our simulations (up to 7 ns).

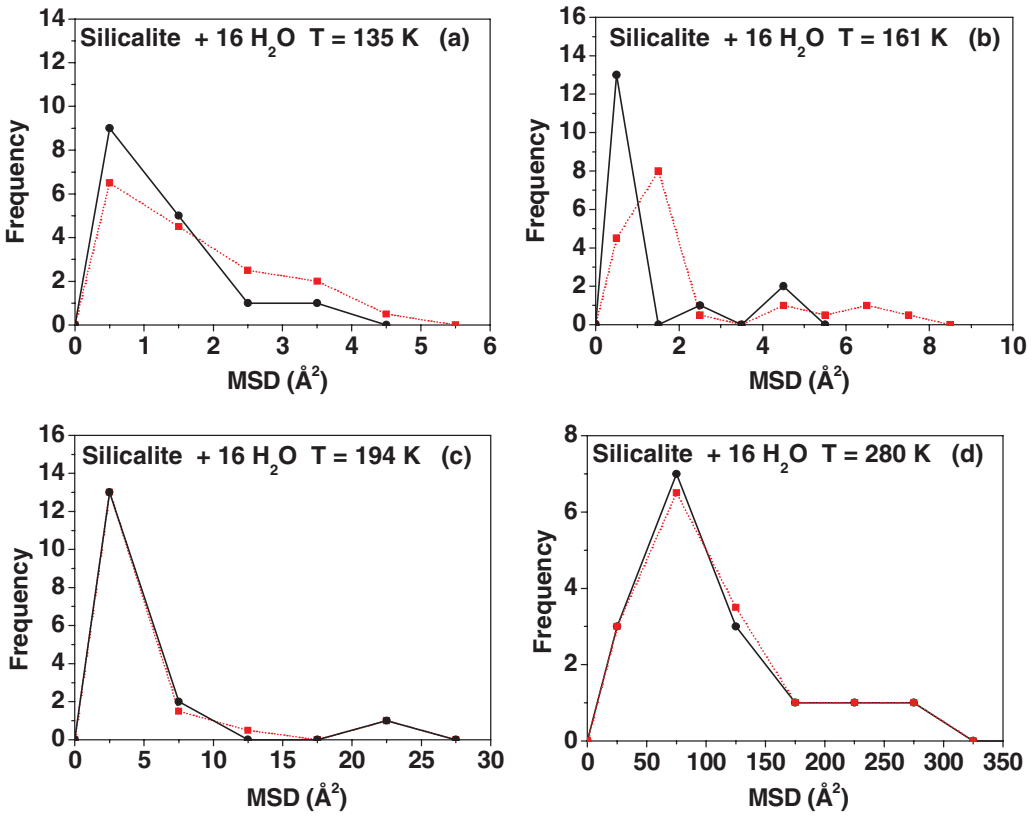

Figure 5. Distributions of MSDs of O atoms (black circles and solid lines) and H atoms (red squares and dotted lines) at some selected temperatures for water in silicalite. Lines are to help guide the eye.

At intermediate temperatures, in the approximate range of 220–280 K, the behaviour of water is almost liquid-like, whereas at higher temperatures there are evidences of vapour-like features [41]. The channel diameter being about 5.5 Å, the water molecules can pass one another but each of them *cannot form more that three HBs*, not even near the channel intersections, where the fourfold coordination is energetically unfavourable in spite of the availability of the required void space.

In figure 3 the distributions of $-\ln C_2(t_0)$ are reported for different temperatures. Their shape and their maxima are strongly temperature dependent. They all show a main peak which is shifted towards higher values of $-\ln C_2(t_0)$ as the temperature increases. This is an expected result, because, according to equation (3), $-\ln C_2(t_0)$ is approximately a linear function of $1/\tau_2$. At very low temperatures, as remarked above, some of the correlation functions decay at a rate higher than the average (corresponding approximately to the main peak), similar to that observed at much higher temperature, resulting in an 'extra tail'. This tail is reduced at higher temperatures, disappears at intermediate (about 200–270 K) and appears again for $T > 280$ K. This trend corresponds to the dynamic behaviour of the clusters adsorbed in silicalite [33, 36, 41].

A synthetic view of this trend is represented in figure 4(*a*), where the percentage of molecules showing values of $-\ln C_2(t_0)$ out of the main peak of the distribution (i.e. the integral of the 'extra tail') against temperature is shown. The second single-molecule property that we considered is the distributions of the MSDs of O and H atoms against temperature. Examples of these distributions for silicalite are shown in figure 5 for selected temperatures, sampling the main different trends. Although in this case the statistics are poor and the histograms are dull, some comments can be attempted. At very low temperature (figures 5(*a*) and (*b*)), at which translational motion (or diffusion) is frozen but some rotational motion is allowed, the distributions of the H atom MSDs will extend to values larger than those of O atoms. Then, as the temperature is increased and diffusion sets on, the two distributions will become indistinguishable (figures 5(*c*) and (*d*)).

Therefore, the disappearance of the excess of the distribution function of H atoms for values of MSDs beyond the main peak of O atoms will show the onset of the diffusion, and other details of its trend will be related to the dynamic crossovers, as will be shown below. In addition, more information can be derived from the shape of the distributions. A main peak will always be present, corresponding to the average behaviour of the adsorbed molecules, but secondary peaks, or extra tails, will indicate diffusive jumps or dynamic heterogeneities.

In figure 4(*b*) the excess of the distribution function of H atoms for values of MSDs beyond the main peak of O atoms versus temperature is plotted. This distribution function shows some anomalies in correspondence with the dynamic crossover temperatures, as derived from the Arrhenius plot of the rotational relaxation constants [36]—namely a shoulder at LTDC and reaching zero value at HTDC.

As discussed in [33, 36], LTDC should correspond to the freezing of the translational motion; it is reasonable that there is a slight bump of the excess rotational motion at that

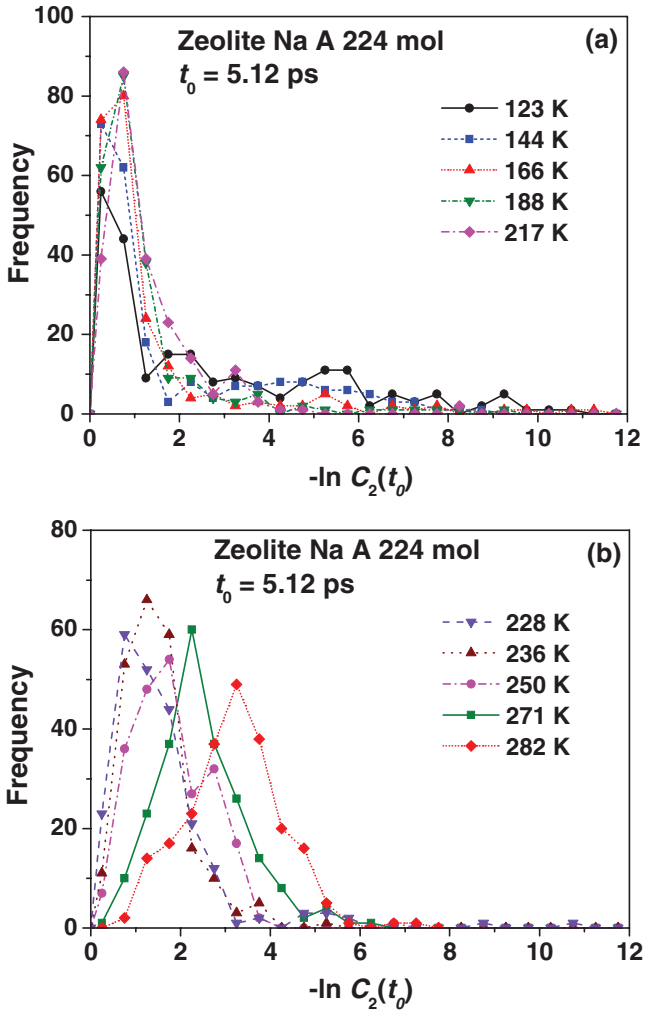

Figure 6. Distributions of $-\ln C_2(t_0)$ at different temperatures, for water in Zeolite Na A. (*a*) Lower temperature range; (*b*) higher temperature range. Lines are to help guide the eye.

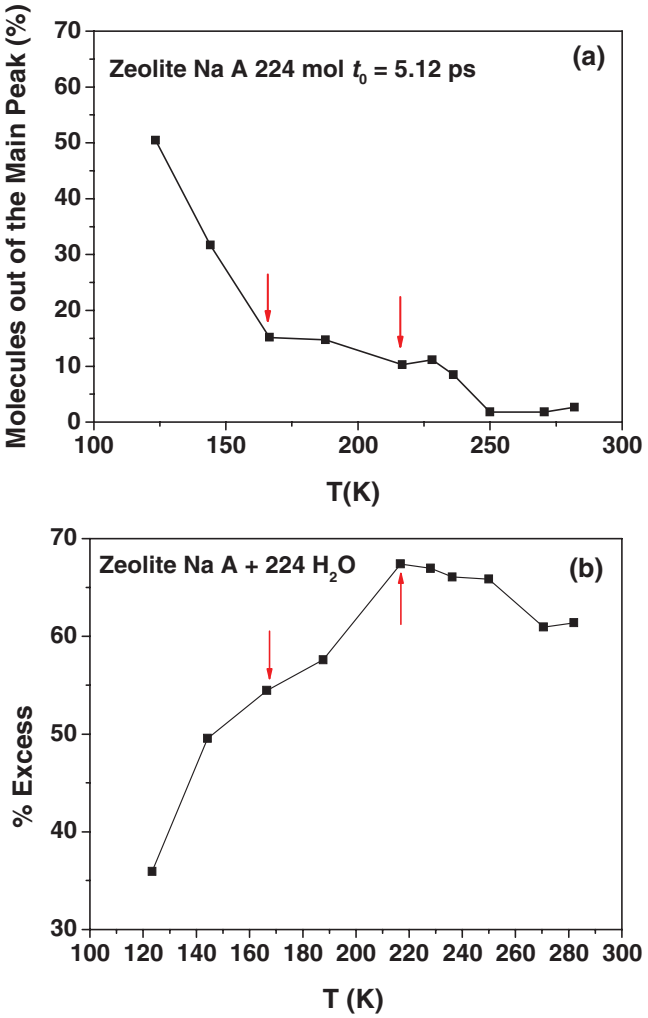

Figure 7. General trends of the distributions of single-molecule properties for Zeolite Na A. (*a*) Percentage of molecules showing values of $-\ln C_2(t_0)$ out of the main peak of the distribution against temperature. (*b*) Percentage of molecules showing a distribution of H atom MSDs larger than that of O atoms out of the main peak of the distribution against temperature. The red arrows show the dynamic crossover temperatures as derived from the Arrhenius plot of the rotational relaxation constants (see figure 1). Lines are to help guide the eye.

temperature. On the other hand, HTDC should correspond to the transition between strong liquid-like behaviour (at lower temperature) and fragile liquid-like (at higher temperature), for which rotational and translational motion are no more decoupled. It is evident that, from figure 4 alone the dynamic crossover temperatures could not be derived. Nevertheless, consideration of the single-molecule properties undoubtedly helps when discussing the molecular mechanism of the dynamic crossovers. We stress that the above discussion is weakened by the poor statistics and that figures 2–5 alone would not furnish a sound basis for any conclusion without previous knowledge of the system's behaviour, which is in agreement. However, it shows the line of reasoning we are following in this study. Subsequent examples will rely on better statistics.

3.2 Zeolite Na A

The MD simulations of Zeolite Na A were performed at full hydration, corresponding to 224 water molecules per unit cell, distributed in 16 clusters [42]. The eight clusters contained in the larger interconnected α-cages (about 12 Å in diameter) include 24 molecules, most of which are coordinated to the Na cations located on the internal surface of the cages. Water molecules can diffuse by crossing the six narrow windows connecting adjacent α-cages. The eight smaller β-cages can contain only four water molecules each, and these molecules can escape from the cages only at high temperature (experimentally for $T > 432$ K), much higher than the temperature range considered in this study (120–270 K).

In the lower temperature range, about 120–220 K (figure 6(*a*)), extended extra tails are evident in the distributions of $-\ln C_2(t_0)$, whereas in the higher temperature range, about 220–270 K (figure 6(*b*)), there are no extra peaks—at most one. One can explain this trend by considering that at low temperature there is a dynamic heterogeneity between the more hindered molecules, coordinated to the Na cations, and the other molecules, whereas at higher temperatures

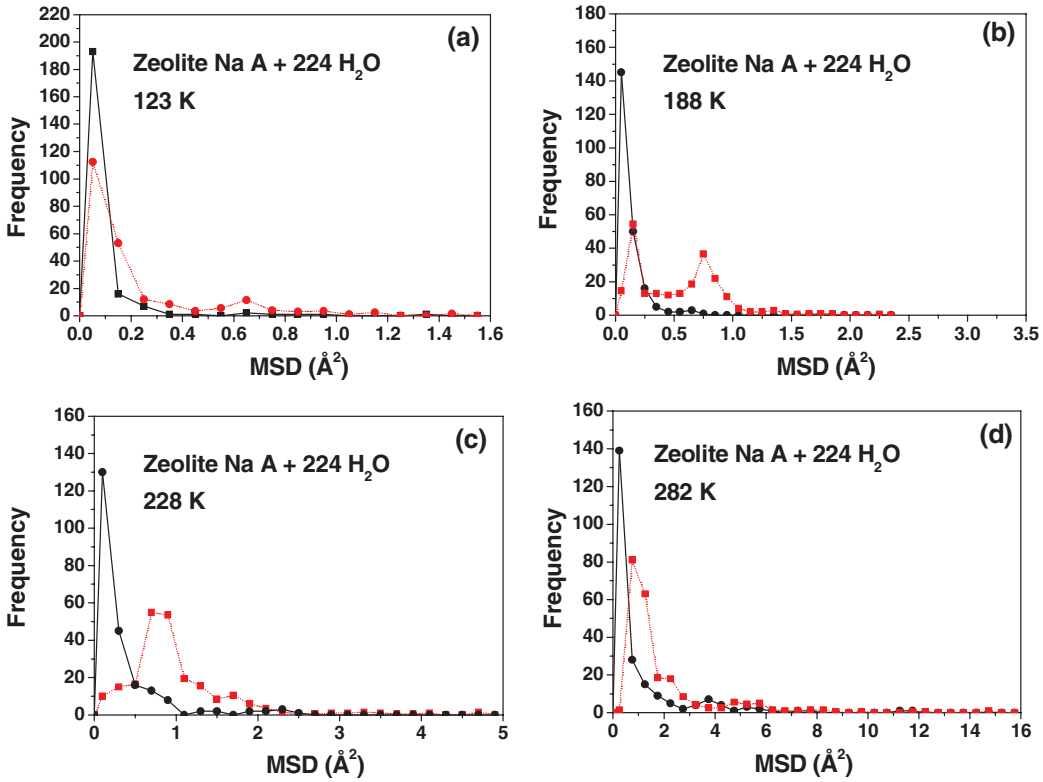

Figure 8. Distributions of MSDs of O atoms (black circles and solid lines) and H atoms (red squares and dotted lines) at some selected temperatures for water in zeolite Na A. Lines are to help guide the eye.

the kinetic energy is sufficiently high to cross the rotational energy barrier, so water's dynamic behaviour becomes more homogeneous. Yet, shoulders or small extra peaks are still present because full homogeneity has not been reached.

In particular, the small tail visible for $-\ln C_2(t_0) \geq 4$ should be attributed to the small number of molecules located near the centre of the cages, which are not coordinated to any cation and are freer to rotate. In an even more refined analysis one could explain why, in figure 6(*b*), the tail is more extended at low than at high temperature. Indeed, at low temperature the water molecules coordinated to the cations stick more tightly to the cations themselves, making more space available to the molecules present in the centre of the cages.

In figure 7(*a*) the data discussed above are summarized as the percentage of molecules showing values of $-\ln C_2(t_0)$ out of the main peak of the distribution against temperature. It is interesting to remark that the dynamic crossover temperatures roughly correspond to *minima* of the line. This finding can be explained by considering that the dynamic crossovers correspond to a change in the distribution of kinetic energy (thus a mixing) between translational and rotational degrees of freedom and therefore a more uniform dynamic landscape.

The MSD of O and H atoms at some selected temperatures is shown in figure 8. The trend is different from that observed in silicalite, because in the considered temperature range diffusion is very slow and only a few molecules jump to another equilibrium position in nanosecond-scale MD simulations.

What changes appreciably are the distribution functions of MSD for H atoms, showing two main peaks: the translational peak (at about 0.15–0.25 Å^2 depending on the temperature), which is superimposed to that of O atoms, and the rotational peak, corresponding to HB exchange (at about 0.7–1.2 Å^2). It should be remarked that if an atom performs one sudden jump of length l at a time $0 < t_0 < t_{max}$, where t_{max} is the duration of the trajectory, its MSD is less than l^2 because l^2 is averaged over all the trajectory and the MSD of the atom for $t < t_0$ (oscillation around equilibrium position) is significantly smaller than l^2.

At very low temperature (120 K) the translational peak is much higher than the rotational ones but, as the temperature is raised, the height of the two peaks is gradually exchanged and both are shifted to higher values of MSD. The latter effect is caused obviously by the thermal amplitude increasing, and the former is due to the rising importance of the rotational motion of the water molecules. At the highest temperatures secondary peaks, corresponding to diffusive jumps (for MSD values larger about than 5 Å^2), begin to appear. As in silicalite, we evaluated the excess of the distribution function of H atoms for values of MSDs beyond the main peak of O atoms versus temperature, which is reported in figure 7(*b*). At the temperatures corresponding to the dynamic crossovers this excess distribution shows a flex point for LTDC and a maximum for HTDC. They can be explained by considering that at LTDC it is reasonable that the mixing of the rotational and translational degrees of freedom dump the excess rotational motion at that temperature. On the other hand, at HTDC rotational motion begins to be coupled to the translational one, as it appears from the rising of a second translational peak in the distribution of oxygens corresponding to the rotational peak of hydrogens in figure 8. At higher temperatures, the appearance of diffusion peaks of oxygens diminishes the excess distributions of hydrogens.

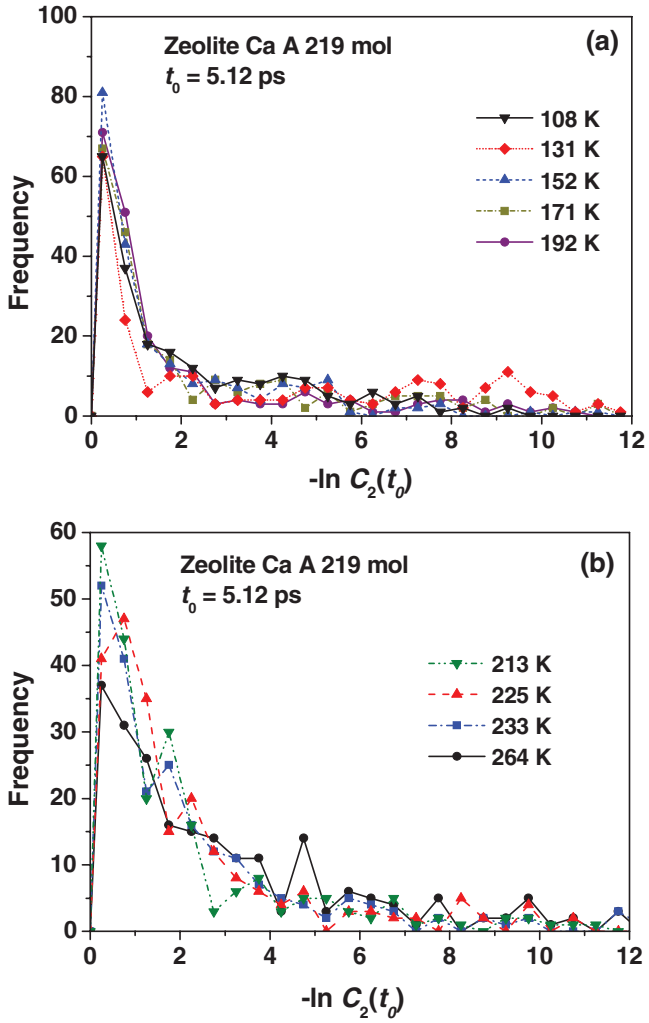

Figure 9. Distributions of $-\ln C_2(t_0)$ at different temperatures for water in Zeolite Ca A. (*a*) Lower temperature range; (*b*) higher temperature range. Lines are to help guide the eye.

3.3 Zeolite Ca A

In Zeolite Ca A, where the Na cations are exchanged with half the number of Ca cations, the behaviour of the water molecules is tightly coordinated with Ca cations, which are only six per α-cage and cannot diffuse, even at high temperature [56]. This is markedly different from that of the other molecules, which are more free both to rotate and translate. Therefore, in the distributions of $-\ln C_2(t_0)$ one should expect extended tails at any temperature, as indeed is the case in figure 9.

In figure 10 the distributions of MSDs of O and H atoms, at some selected temperatures, is reported. The trend is similar to that of zeolite Na A but diffusion is slower at any temperature and only a few molecules perform diffusive jumps in nanosecond-scale MD simulations.

As in Zeolite Na A (see figure 8) the distribution function of MSD for H atoms, shows two main peaks: the translational peak (at about 0.1 Å^2 depending only slightly on temperature), which is superimposed to that of O atoms, and the rotational peak, corresponding to HB exchange (at about 0.7 Å^2 practically independent of temperature).

Again, as in Zeolite Na A, at very low temperature (120 K) the translational peak is much higher than the rotational ones, but raising the temperature causes the height of the two peaks gradually to be exchanged. At the highest temperatures secondary peaks, corresponding to diffusive jumps for MSD values of about 5 Å^2, are visible. The excess of the distribution function of H atoms for values of MSDs beyond the main peak of O atoms versus temperature is reported in figure 11(*b*). The temperatures of the dynamic crossovers correspond to a minimum of the distribution for LTDC (against a flex point in zeolite Na A) and to a maximum for HTDC, but the interpretation of the trend can be the same.

It is not possible to extract useful information about dynamical crossovers directly from figure 9, but, as in the previous cases, one can consider the percentage of molecules showing values of $-\ln C_2(t_0)$ out of the main peak of the distribution against temperature that is plotted in figure 11(*a*). The two minima correspond to the dynamic crossover temperatures, a signature of the mixing between translational and rotational degrees of freedom and therefore a relatively uniform dynamic landscape. As the number of the Ca cations in zeolite Ca A is one half of that of Na cations in zeolite Na A, the number of water molecules directly coordinated to the cations is also smaller, namely 158, assuming that the coordination corresponds to a Ca–O distance smaller than the one corresponding to the first minimum in the Ca–O radial distribution function (RDF), or 3.5 Å. We evaluated the single-molecule properties of the water molecules coordinated to the cations and the 'free' molecules (61 in number) and, indeed, the latter showed a larger mobility, especially at high temperature. This was as expected because, at low temperature, the motion is hindered even by lower energy barriers.

3.4. Zeolite Na X

The size of the cages of zeolite Na X is similar to those of zeolite A. But they are tetrahedrally connected by larger windows, about 7.5 Å in diameter, so that water molecules are less hindered. Indeed, at room temperature the diffusion coefficient is only one order of magnitude smaller than in bulk water at full hydration [43], and the average rotational relaxation constants are similar, or even *larger*, than in bulk water at the considered temperature range [33]. This happens because some Na cations are not accessible to water molecules and the HBs formed with the zeolite surface are weaker than the intermolecular ones.

As a consequence, the distributions of $-\ln C_2(t_0)$ show tails at low temperature only, where most molecules are translationally frozen and a few of them are rotationally less hindered (see figure 12(*a*)). As the temperature is raised the rotational motion becomes more and more uniform and the distributions of $-\ln C_2(t_0)$ become Gaussian-like and remarkably narrow, although a small percentage of molecules—with rotational constant values not belonging to the main peak—are still present (see figure 12(*b*)).

Figure 13(*a*) shows the percentage of molecules with values of $-\ln C_2(t_0)$ out of the main peak of the distribution against

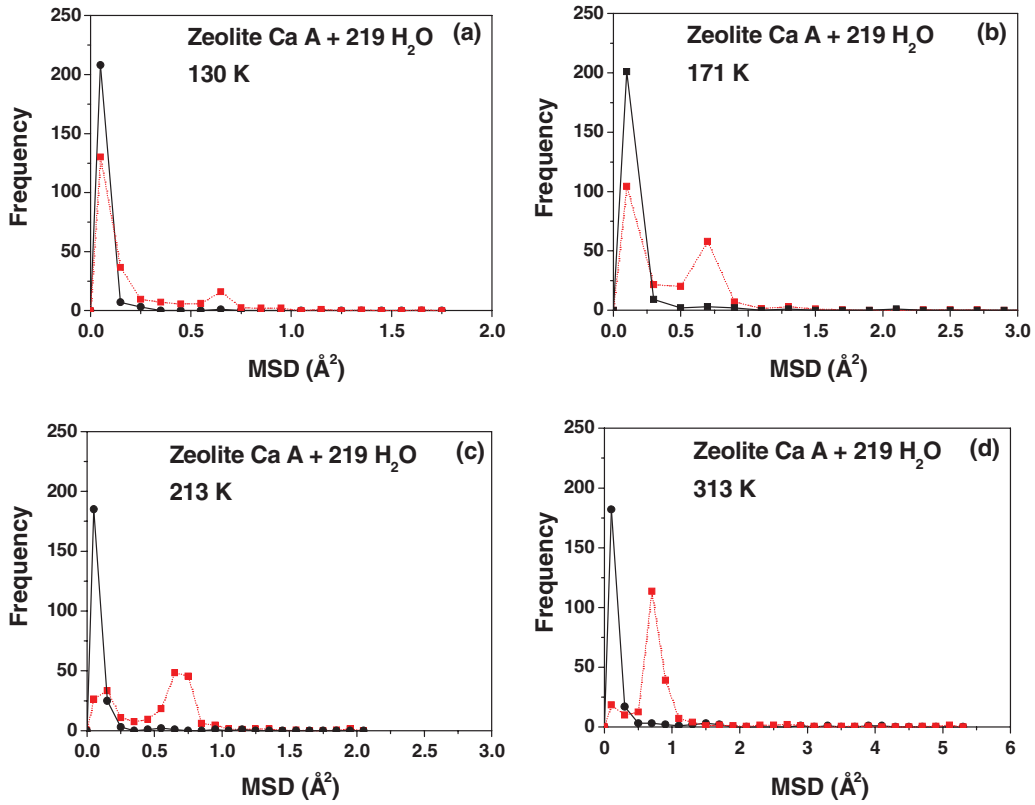

Figure 10. Distributions of MSDs of O atoms (black circles and solid lines) and H atoms (red squares and dotted lines) at some selected temperatures for water in zeolite Ca A. Lines are to help guide the eye.

temperature. Two minima, corresponding to the dynamic crossover temperatures, are visible, indicating mixing between translational and rotational degrees of freedom and therefore a relatively uniform dynamic landscape at the crossovers.

The distributions of MSD of O and H atoms at some selected temperatures is reported in figure 14. At very low temperature the MSD of most atoms does not exceed about 0.2 Å^2, slightly larger for H atoms, as should be expected because at least some molecules possess a rotational motion. At temperatures close to the LTDC (just above) the H atoms show an excess MSD frequency, although the values do not represent diffusive jumps, except for a very small number of molecules. At about 233 K (just above the HTDC), the distribution of H and O atoms is decoupled, but diffusive jumps are still negligible. Finally, at room temperature diffusion is predominant and the distributions become practically superimposed. The excess of the distribution function of H atoms for values of MSDs beyond the main peak of O atoms versus temperature (plotted in figure 13(*b*)) as in zeolite Ca A shows a minimum corresponding to the LTDC and a maximum to HTDC, the interpretation of the trend being the same.

4. Conclusions

In this contribution we have used an approach to single out the heterogeneous dynamic behaviour of confined liquids based on estimating dynamic single-molecule properties. The probability distribution of such properties are computed by MD simulations sufficiently long to ensure a good sampling and to reduce errors. While systems characterized by homogeneous dynamics are expected to show a narrow Gaussian distribution, interesting information is gained by inspecting the patterns arising in heterogeneous systems. In particular we have applied a method to deepen the understanding of the dynamic behaviour of water adsorbed in zeolites, focusing mainly on dynamics heterogeneities and on the mechanisms of dynamic crossovers at the molecular level. We have thus characterized the dependence on the shape and size of different channels and cavities, and on the concentration of cations. For example, we furnish a clear-cut explanation, and a more general picture, of the differences in the activation energy for water rotational motion among zeolites Ca A and Na A, that was previously done by invoking different hydration of the cations [33]. We consider this method as complementary to the study of collective (average) properties for a complete understanding of the behaviour of nanoconfined water, especially for a comparison to experimental data. One can confirm substantially the conclusion drawn about the nature of the of *two dynamic crossovers*: HTDC (in the temperature range 200–230 K) and LTDC (in the temperature range 150–185 K). The molecular level mechanism invoked in [33] to explain HTDC is the formation of translationally rigid clusters [4, 5], allowing however some rotational freedom, including HB exchange. Indeed we did not obtain a value of the diffusion coefficient of water adsorbed in zeolites in the supercooled regime, except for silicalite [41] (see also figure 5), because

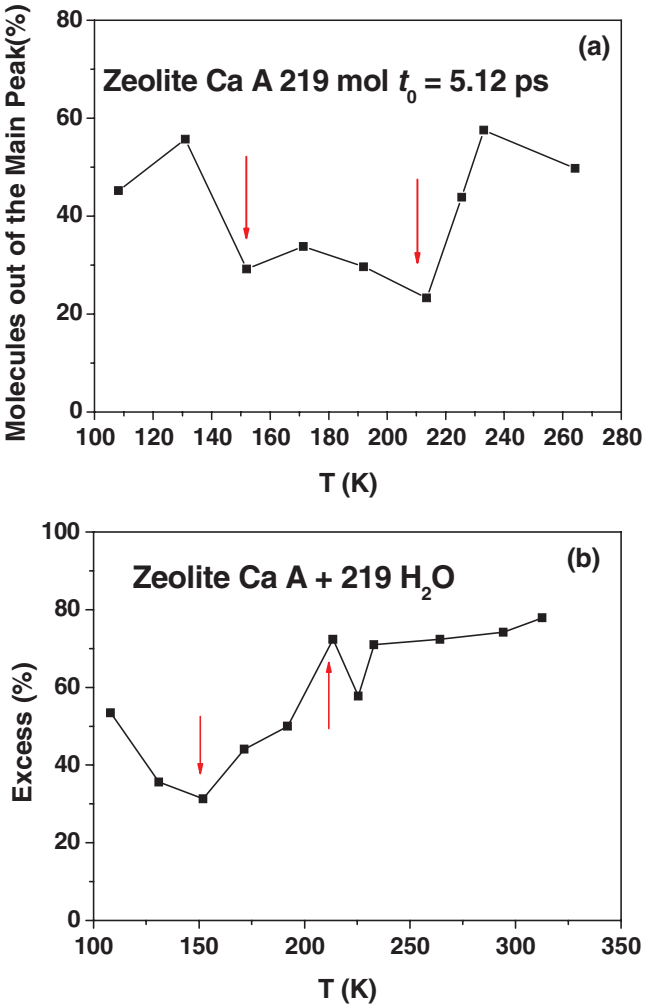

Figure 11. General trends of the distributions of single-molecule properties for Zeolite Ca A. (*a*) Percentage of molecules showing values of $-\ln C_2(t_0)$ out of the main peak of the distribution against temperature. (*b*) Percentage of molecules showing a distribution of H atom MSDs larger than that of O atoms out of the main peak of the distribution against temperature. The red arrows show the dynamic crossover temperatures as derived from the Arrhenius plot of the rotational relaxation constants (see figure 1). Lines are to help guide the eye.

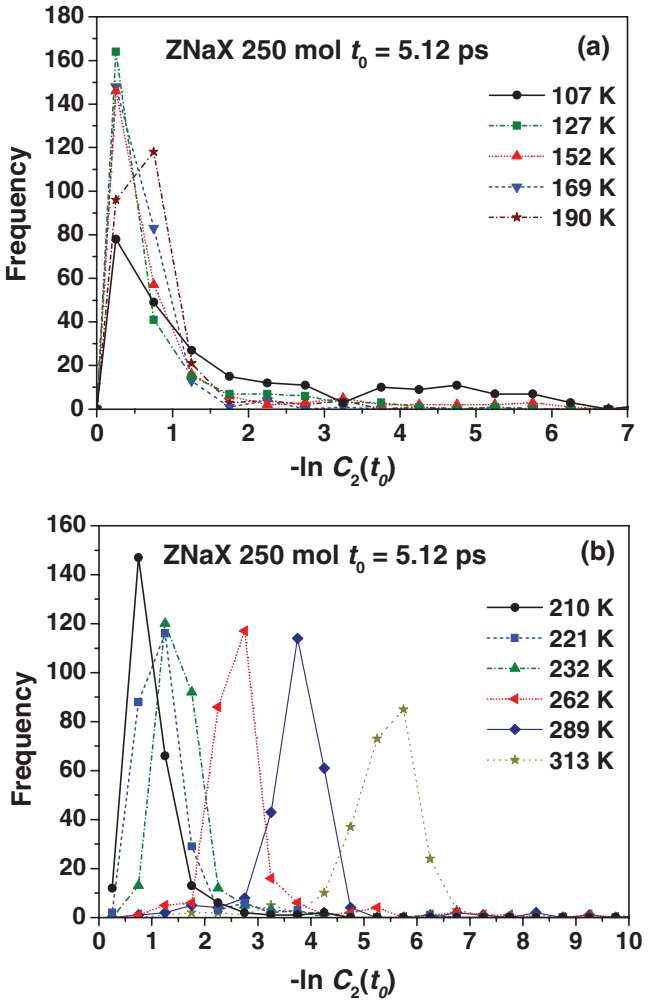

Figure 12. Distributions of $-\ln C_2(t_0)$ at different temperatures for water in Zeolite Na X. (*a*) Lower temperature range; (*b*) higher temperature range. Lines are to help guide the eye.

the diffusion coefficient is usually smaller than in bulk water at the same temperature [59], and in most zeolites it is out of the reach of MD simulations. However, even at temperatures below HTDC, when it does not freeze, water still shows a liquid-like behaviour; some diffusion is present also in water adsorbed in zeolites, as can be guessed, not only in figure 5, but also in figure 14(*b*) above. Therefore, the previous statement about the HTDC must be completed by including the diffusive process. This cannot be described by the same concerted rotational–translational mechanism, as in 'fragile' water [26, 28–32] entailing the VFT trend of the translational relaxation constants, because at temperatures below HTDC for the same quantity one observes an Arrhenius trend. Recently, by making very long simulations of supercooled bulk water reaching the microsecond time scale, Picasso *et al* [26] were able to study and discuss the diffusion mechanism down to 200 K. They confirmed the VFT and Arrhenius trends of the average translational relaxation times for temperatures higher and lower than the HTDC, respectively. However, on the basis of a specially designed multi-scale displacement analysis, which is a form of single-molecule distribution, they described the diffusion mechanism at temperatures below the HTDC as due to a sequence of cage-to-cage translational jumps. This process is decoupled from rotational motion and, according to the transition state theory, should follow an Arrhenius trend. A similar decoupling was observed experimentally by Edmond *et al* [60] in tetrahedral clusters suspended in colloidal supercooled fluids, near the colloidal glass transition. In conclusion, the complete interpretation of the HTDC mechanism should read: 'the high temperature dynamical crossover (HTDC) occurring in the temperature range 200–230 K can be interpreted at a molecular level as the formation of translationally almost rigid clusters, permitting however some rotational motion, including HB exchange and translational jumps as cage-to-cage processes'. In order to interpret the LTDC mechanism in [33] it was suggested that 'the adsorbed water clusters are made of nearly rigid sub-clusters, slightly mismatched, thus permitting a relatively free librational motion at their borders'. This mechanism entails,

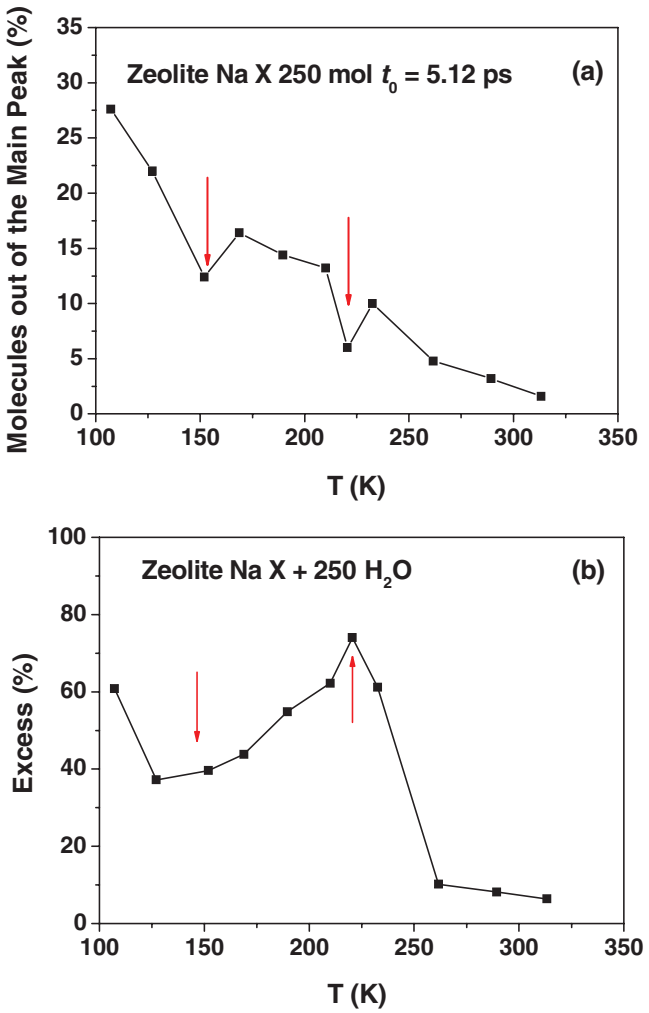

Figure 13. General trends of the distributions of single-molecule properties for Zeolite Na X. (*a*) Percentage of molecules showing values of $-\ln C_2(t_0)$ out of the main peak of the distribution against temperature. (*b*) Percentage of molecules showing a distribution of H atom MSDs larger than that of O atoms out of the main peak of the distribution against temperature. The red arrows show the dynamic crossover temperatures as derived from the Arrhenius plot of the rotational relaxation constants (see figure 1). Lines are to help guide the eye.

for temperatures below the LTDC, that the measured or computed effective rotational activation energy is very low [33], because it is averaged over all the adsorbed molecules, most of which are rotationally frozen. However, the consideration of single-molecule properties allows one to add more details. In addition to the case of silicalite, where the adsorbed clusters do not fill completely the channels and leave isolated or terminal molecules relatively free to rotate, in the other zeolites the less hindered molecules are those not directly coordinated to the cations. Such are, for instance, the few molecules located near the centre of the α-cages in zeolite Na A, or some molecules belonging to the surface of the adsorbed clusters and interacting with the aluminosilicate framework through HBs that are weaker than water–water HBs, such as the molecules close to the windows connecting the cages of zeolites Ca A and Na X. In general, the presence of *two* dynamic crossovers has been found, both by simulations and different experimental techniques, in supercooled water, when it is possible to avoid crystallization through nano-confining or through adsorption on the surfaces of solid porous materials, organic or biological molecules (see [33] for more details). Further recent examples are a study by Mazza *et al* [12], reporting dielectric relaxation experiments and Monte Carlo simulations of hydration water of lysozyme, a globular protein, and another experimental study by Schirò *et al* [61] about hydrated myoglobin discussing experimental data from elastic neutron scattering, broadband dielectric spectroscopy and differential scanning calorimetry. Other examples of systems where nano-confinement of water has been investigated, besides those quoted in [33], are silica nanopores [24, 44, 62–71], nanoporous zeolite-template carbon [25] and reverse micelles [45–47]. In all these cases the adsorbed molecules are subject to highly heterogeneous environments, which allow some dangling HBs or weaker than water–water HBs, so that some dynamics is permitted also at very low temperature, even if most rotational motion is frozen. Also, relatively small solvated organic molecules show strong hydrophobic effects that make the environment sufficiently heterogeneous to permit the onset of the LTDC. Another more general example is a 'translational' LTDC, which was evidenced in a Lennard-Jones monoatomic fluid confined in slit-shaped pores with structured walls [72], and was interpreted as due to 'single particle motion' – arguably the particles belonging to the fluid–wall interface – whose translational dynamics is different from that of the bulk ones. On the contrary, LTDC was not evidenced in high concentration simple salt solutions [73], where there is no extended heterogeneous 'interface' at the border of clusters. As with most rules, at least one exception was found. Indeed, Bove *et al* [74] reported transient grating experiments on supercooled $LiCl(H_2O)_6$ solution which yielded an extra signal below 190 K, interpreted as 'a phase separation between clusters with low solute concentration and the remaining, more concentration, solution'. They also suggest, in line with the above reported interpretation of the LTDC, that the process causing the extra signal 'could be a boundary effect: molecules located at the boundary between a cluster, with its own temperature, and its surrounding with another one, could equilibrate more rapidly their local temperature (kinetic energy) with the liquid matrix than those located inside a cluster.' In other words, the molecules located at a cluster's boundary show a mobility larger than those inside the cluster. The same authors stress that 'none of the studies mentioned so far was concerned with a situation similar to the present one where [...] [in a liquid] coexist phases with different solute concentration'. Similar conclusions are reported in a very recent paper by Sattig and Vogel [75] about ^{2}H NMR experiments detecting two dynamic crossovers of supercooled water confined in a MCM-41 silica material, which exhibits pores with diameters of about 20 nm. We therefore guess that it is unlikely to find this kind of dynamical crossover in supercooled bulk water, because it is a relatively homogeneous system, and the freezing of the rotational freedom of the molecules of the clusters should correspond to the glass transition because the mismatch between clusters [4, 5] probably would not allow the interstitial molecules to rotate.

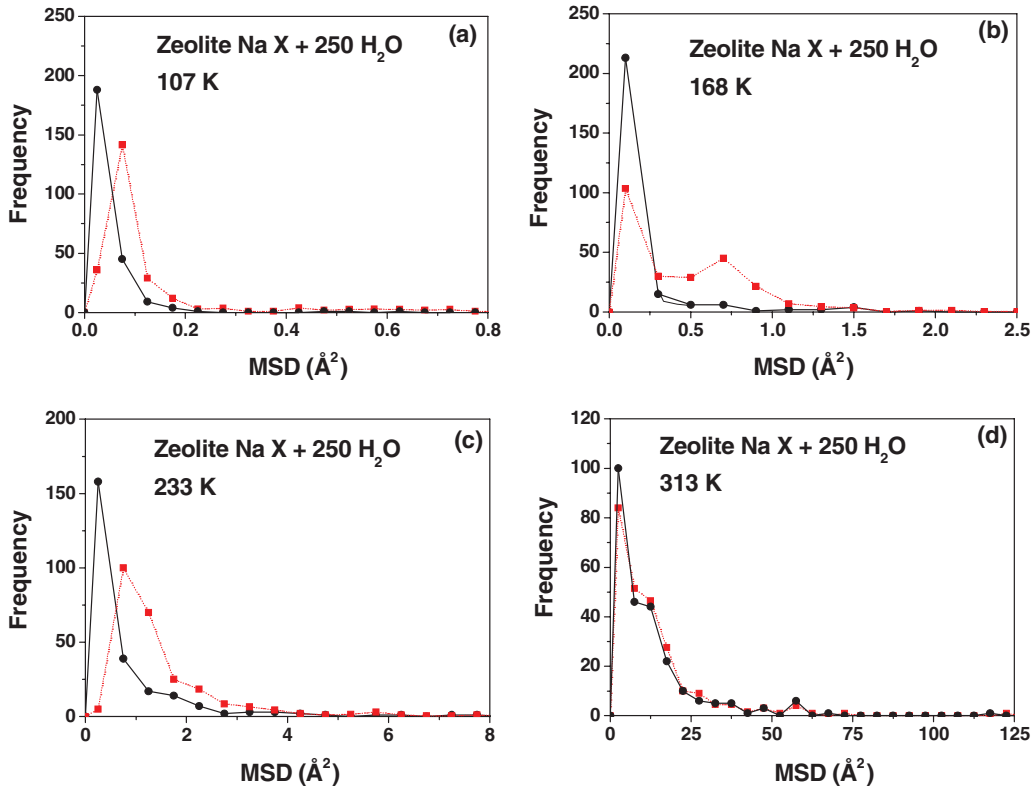

Figure 14. Distributions of MSDs of O atoms (black circles and solid lines) and H atoms (red squares and dotted lines) at some selected temperatures for water in zeolite Na X. Lines are to help guide the eye.

Although LTDC can be facilitated by a heterogeneous environment, taking into account possible quantum effects, *a priori* it cannot be excluded in bulk water, where self-generated heterogeneity could give rise to weaker HBs. We are grateful to one of the referees for this remark. Therefore, our method can be used profitably to investigate the dynamical heterogeneities also in supercooled bulk water. Work is now in progress to extend the simulations to bulk water using different potentials.

Acknowledgments

This research is supported by the Italian Ministero dell'Istruzione, dell'Università, e della Ricerca (MIUR), Regione Autonoma della Sardegna (Italy), Università degli studi di Sassari and Istituto Nazionale per la Scienza e Tecnologia dei Materiali (INSTM), which are acknowledged. The 'Consorzio COSMOLAB' is also acknowledged for resources provided within the CyberSar Project. We are grateful to Professor G Franzese for useful discussion of our results and for the encouragement in continuing our study.

References

[1] Röntgen W C 1892 *Ann. Phys.* **281** 91
[2] La Nave E and Sciortino F 2004 *J. Phys. Chem.* B **108** 19663
[3] Stanley H E, Buldyrev S V, Franzese G, Giovanbattista N and Starr F W 2005 *Phil. Trans. R. Soc.* A **363** 509
[4] Matharoo G S, Razul M S G and Poole P H 2006 *Phys. Rev.* E **74** 050502(R)
[5] Kumar P, Buldyrev S V, Becker S R, Poole P H, Starr F W and Stanley H E 2007 *Proc. Natl Acad. Sci. USA* **104** 9575
[6] Mazza M G, Giovanbattista N, Stanley H E and Starr F W 2007 *Phys. Rev.* E **76** 031203
[7] Stanley H E, Kumar P, Han S, Mazza M G, Stokeley K, Buldyrev S V, Franzese G, Mallamace F and Xu L 2009 *J. Phys.: Condens. Matter* **21** 504105
[8] Stokeley K, Stanley H E, Mazza M G and Franzese G 2010 *Proc. Natl Acad. Sci. USA* **107** 1301
[9] Sedlmeier F, Horinek D and Netz R R 2011 *J. Am. Chem. Soc.* **133** 1391
[10] Shajahan M, Razul G, Matharoo G S and Poole P H 2011 *J. Phys.: Condens. Matter* **23** 235103
[11] Nilsson A and Pettersson L G M 2011 *Chem. Phys.* **389** 1
[12] Mazza M G, Stokeley K, Pagnotta S E, Bruni F, Stanley H E and Franzese G 2011 *Proc. Natl Acad. Sci. USA* **108** 19873
[13] Teixeira J 2011 *Mol. Phys.* **110** 249
[14] Grzybowski A, Kolodziejczyk K, Koperwas K, Grzybowska K and Paluch M 2012 *Phys. Rev.* B **85** 220201(R)
[15] Lupi L, Comez L, Paolantoni M, Fioretto D and Ladanyi B M 2012 *J. Phys. Chem.* B **116** 7499
[16] Hentschel H G E, Karkamar S, Procaccia I and Zylberg J 2012 *Phys. Rev.* E **85** 061501
[17] Elmatad Y S and Keys A S 2012 *Phys. Rev.* E **8** 061502
[18] Sussman D M and Schweizer S 2012 *Phys. Rev.* E **85** 061504
[19] Liao Y, Yang S K, Koh K, Matzger A J and Biteen J 2012 *Nano Lett.* **12** 3080
[20] Bomont J-M, Bretonnet J-L, Costa D and Hansen J-P 2012 *J. Chem. Phys.* **137** 011101
[21] Prada-Gracia D, Shevchuk R, Hamm P and Rao F 2012 *J. Chem. Phys.* **137** 144504
[22] Stirnemann G and Laage D 2012 *J. Chem. Phys.* **137** 031101
[23] Moore E B and Molinero V 2009 *J. Chem. Phys.* **130** 244505

[24] Laage D and Thompson W H 2012 *J. Chem. Phys.* **136** 044513
[25] Kyakuno H, Matsuda K, Nakai Y, Fukuoka T, Maniwa Y, Nishihara H and Kyotani T 2013 *Chem. Phys. Lett.* **571** 54
[26] Picasso G C, Malaspina D C and Carignano M A 2013 *J. Chem. Phys.* **139** 044509
[27] Khamzin A A, Popov I I and Nigmatullin R R 2013 *J. Chem. Phys*. **138** 244502
[28] Laage D and Hynes J T 2006 *Science* **311** 832
[29] Laage D and Hynes J T 2008 *J. Phys. Chem.* B **112** 14230
[30] Laage D, Stirnemann G, Sterpone F and Hynes J T 2012 *Acc. Chem. Res*. **45** 53
[31] Laage D, Stirnemann G, Sterpone F, Rey R and Hynes J T 2011 *Annu. Rev. Phys. Chem.* **62** 395
[32] Liu Ch, Li W and Wang W 2013 *Phys. Rev.* E **87** 052309
[33] Demontis P, Gulín-González J, Masia M and Suffritti G B 2012 *J. Phys.: Condens. Matter* **24** 064110
[34] Widmer-Cooper A, Harrowell P and Fynewever H 2004 *Phys. Rev. Lett*. **93** 135701
[35] Candelier R, Widmer-Cooper A, Kummerfeld J K, Dauchot O, Biroli G, Harrowell P and Reichman D R 2010 *Phys. Rev. Lett*. **105** 135702
[36] Demontis P, Gulín-González J, Masia M and Suffritti G B 2010 *J. Phys.: Condens. Matter* **22** 284106
[37] Frenkel D and Smit B 2002 *Understanding Molecular Simulations: from Algorithms to Applications* 2nd edn (San Diego, CA: Academic)
[38] Beck D W 1974 *Zeolite Molecular Sieves* (New York: Wiley)
[39] Barrer R M 1978 *Zeolites and Clay Minerals as Sorbents and Molecular Sieves* (London: Academic)
[40] van Bekkum H, Flanigen E M, Jacobs P A and Jansen J C (ed) 2001 *Introduction to Zeolite Science and Practice; Studies in Surface Science and Catalysis* 2nd edn, vol 137 (Amsterdam: Elsevier)
[41] Demontis P, Stara G and Suffritti G B 2003 *J. Phys. Chem.* B **107** 4426
[42] Demontis P, Gulín-González J, Jobic H, Masia M, Sale R and Suffritti G B 2008 *ACS Nano* **2** 1603
[43] Demontis P, Gonzalez M A, Jobic H and Suffritti G B 2009 *J. Phys. Chem.* C **113** 12373
[44] Milischuk A M and Ladanyi B M 2011 *J. Chem. Phys*. **135** 174709
[45] Harpham M R, Ladanyi B M, Levinger N E and Herwig K W 2004 *J. Chem. Phys*. **121** 7855
[46] Harpham M R, Ladanyi B M and Levinger N E 2005 *J. Phys. Chem.* B **109** 16891
[47] Rodriguez J, Laria D, Guàrdia E and Martí J 2009 *Phys. Chem. Chem. Phys*. **11** 1484
[48] Dokter A M, Petersen C and Bakker S H 2008 *J. Chem. Phys.* **128** 044509
[49] Pradzynki C C, Forck R M, Zeuch T, Slavíček P and Buck U 2012 *Science* **337** 1529
[50] Guillot B and Guissani Y 1998 *J. Chem. Phys.* **108** 10162
[51] Hernández de la Peña L and Kusalik P G 2004 *J. Chem. Phys.* **121** 5992
[52] Hernández de la Peña L and Kusalik P G 2005 *J. Am. Chem. Soc.* **127** 5246
[53] Jansson H and Swenson J 2003 *Eur. Phys. J.* E **12** S51
[54] Swenson J, Jansson H and Bergman R 2006 *Phys. Rev. Lett.* **96** 247802
[55] Swenson J, Jansson H, Howells W S and Longeville S 2005 *J. Chem. Phys.* **122** 084505
[56] Demontis P, Gulín-González J, Jobic H and Suffritti G B 2010 *J. Phys. Chem.* C **114** 18612
[57] Gordon R G 1968 *Advances in Magnetic Resonance* vol 3, ed J S Waugh (New York: Academic) p 1
[58] Zasetsky A Y 2011 *Phys. Rev. Lett*. **107** 117601
[59] Paoli H, Méthivier A, Jobic H, Krause C, Pfeifer H, Stallmach F and J Kärger 2002 *Microp. Mesop. Mater.* **55** 147
[60] Edmond K V, Elsesser M T, Hunter G L, Pine D J and Weeks E R 2012 *Proc. Natl Acad. Sci. USA* **109** 17891
[61] Schirò G., Fomina M and Cupane A 2013 *J. Chem. Phys*. **139** 121102
[62] Rovere M, Ricci M A, Vellati D and Bruni F 1998 *J. Chem. Phys*. **108** 9859
[63] Gallo P, Rovere M and Spohr E 2000 *J. Chem. Phys*. **113** 11324
[64] Gallo P 2000 *Phys. Chem. Chem. Phys.* **2** 1607
[65] Gallo P, Rapinesi M and Rovere M 2002 *J. Chem. Phys.* **117** 369
[66] Gallo P, Ricci M A and Rovere M 2002 *J. Chem. Phys.* **116** 342
[67] Gallo P and Rovere M 2003 *J. Phys.: Condens. Matter* **15** 7625
[68] Yoshida K, Yamaguchi T, Kittaka S, Bellissent-Funel M-C and Fouquet P 2008 *J. Chem. Phys*. **129** 054702
[69] Gallo P, Rovere M and Chen S-H 2010 *J. Phys. Chem. Lett.* **1** 729
[70] Gallo P, Rovere M and Chen S-H 2010 *J. Phys.: Condens. Matter* **22** 284102
[71] Kittaka S, Takahara S, Matsumoto H, Wada Y, Satoh T J and Yamaguchi T 2013 *J. Chem. Phys.* **138** 204714
[72] Krishnan S H and Ayappa K G 2012 *Phys. Rev. E* **86** 011504
[73] Santucci S C, Comez L, Scarponi F, Monaco G, Verbeni R, Legrand J-F, Masciovecchio C, Gessini A and Fioretto D 2009 *J. Chem. Phys.* **131** 154507
[74] Bove L E, Dreyfus C, Torre R and Pick R M 2013 *J. Chem. Phys.* **139** 044501
[75] Sattig M and Vogel M 2014 *J. Phys. Chem. Lett.* **5** 174